UNIVERSITY OF TROMSØ UIT

FACULTY OF SCIENCE AND TECHNOLOGY
DEPARTMENT OF PHYSICS AND TECHNOLOGY

Spectral analysis of radar coherent echoes and its relation to turbulence

Marshal Pokhrel

FYS-3900 Master's Thesis in Physics

November 2012

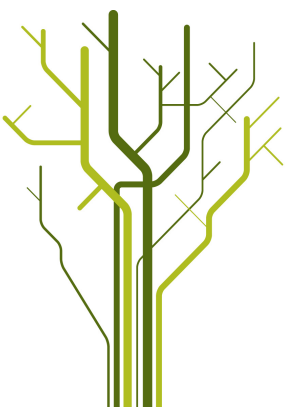

Spectral analysis of radar coherent echoes and its relation to turbulence

A Thesis Submitted by:

Marshal Pokhrel

Master in Physics
Faculty of Science and Technology
University of Tromsø

Supervised by:

Dr.Cesar La Hoz

University of Tromsø
Norway

Acknowledgement

I would like to thank my advisor in this whole work, Dr. Cesar La Hoz, for many ideas and instructions that he had provided during this work. I would like to thank him for his co-operation and dedication to bring my thesis to an end. Many useful suggestions and comments on my work by him had given my thesis a final shape. In addition to that, I am really fortunate to know the phenomena PMSE(Polar Mesosphere Summer Echoes) and its characteristics, and I appreciate him for providing me an opportunity to learn and know about it.

I would like to express my gratitudes to the University of Tromso for offering me to study masters and for providing me all the facilities that I need.

Heartly regards to all my friends who had helped me and had inspired me during my work without whom the work would have been difficult to be made.

Last but not the least, I am thankful to my family members for being supportive and respecting my decision that I have taken in my life.

Marshal Pokhrel

November 2012

Abstract

The measurements of polar mesosphere summer echoes has been performed since a long time by the ground based techniques with European Incoherent Scatter Scientific Association(EISCAT) Very high frequency(VHF) and Ultra high frequency(UHF) radar system and recently with MORRO. Based on these observation, my thesis is focussed on the data obtained from manda program to get data from EISCAT 3D demonstrator antenna array in Kiruna that receives from EISCAT VHF transmitter here from Tromso in the year July 2011 to analyse the Polar Mesospheric Summer Echoes(PMSE). The thesis starts with the data analysis of the PMSE observing its parameters like spectral width, doppler shift and amplitude. These parameters are built in a profile and plotted as a function of time and height. In addition, the widely accepted fact of the dependence of PMSE with turbulence is shown in the thesis which is made by showing the profiles of dissipation rate as a function of height and time. Focus is made on calculation of spectral width and its variations with height in different times. In addition , the dissipation rate has been depicted and the physics underlying beneath it has been explained.

Contents

List of Figures

Chapter 1

Background and structure of the thesis

Research and investigation in space science has contributed a lot of better understanding about the earth atmosphere. Still, there are ongoing research in this area to contribute even more .With an idea to know about atmosphere, my thesis aims at understanding the phenomena called Polar mesosphere summer echoes to some extent. Knowing it nature, its variability and its origin and the factor influencing such echoes will be discussed. Besides , some statistical properties will be found out and will be discussed.

- **Structure of this thesis**

  This thesis will mainly focus on the analysing the experimental data from EISCAT radar located near Tromso. These datas are taken out from the enhanced echoes in summer from mesosphere at polar region namely called as mesospheric echoes. From the constant research and investigations, it has been known that the air turbulence with charged ice particles that induces the electron density are producing such enhanced echoes. I will be calculating the spectral widths of these spectrums and finding the dissipation rate and the physics behind. Thus the result so obtained can be made useful to investigate the physical properties of turbulence associated with the radar echoes.

  The second chapter will basically talk about the structure of atmosphere, the profile of temperature and some phenomenas occurring there.

  The third chapter of this thesis will talk about causes of PMSE, its dynamical characteristics and different phenomenas associated with it. There are various interesting phenomenas that are found associated with PMSE and some of them , for example Noctulicent clouds(NLC) are found in the vicinity of mesopause , thereby suggesting us the correlation of the occurence of these two different phenomenas.

  The fourth chapter will briefly throw a light upon the theory of PMSE. This chapter

will explain the origin of PMSE and its dependency on various factors. The role of turbulence will be described in this chapter.

The fifth chapter will be on the theory of radar techniques and principles, reflections mechanisms. Theories about incoherent scattering and a brief introduction to EISCAT will be given. This chapter will be mainly focussed to acknowledge the background of radar techniques.

The sixth chapter will mainly focus on the methods used to analysis the obtained data from EISCAT.This chapter of this thesis will mainly be focussed on the data simulation and analysis using the provided mathematical tool called Mathematica and JAVA. The work is mainly to determine the spectral width of such produced enhanced summer echoes and have a idea about the dissipation rates.

Seventh chapter covers the result of the analysis. Obtained results from the analysis will help us to know to see the relation of width of the spectrum and intensity of turbulence. The footprints of turbulence can be seen in the spectral shape which will be shown in the results in this chapter.

Finally, in the eight chapter the conclusion of the whole thesis and the future aspects will be given.

Chapter 2

Structure of mesosphere

2.1 Introduction

Indeed since the beginning of time, atmosphere has always been a place of mystery for scientists and researchers. Recently, it has been observed that the effect from traces of gases from human activity has changed the dynamics of the upper atmosphere to a certain extent. Relatively, the understanding of the upper atmosphere is less in comparison to the lower atmosphere. In this thesis, the content is focussed in the upper layer of the atmosphere, and it is worth explaning its temperature variability. Besides that, we will be explaning the dynamical characteristics and different phenomenas such as NLC, charged aerosols and gravity waves associated with PMSE.

2.2 Layers of the atmosphere

Generally, the atmosphere is divided in to different layers as according to the temperature profile which varies in different ways. For instance we can have a feeling, that as we go up, the temperature decreases in comparision to the lower layers and which is true to some extent.

The first layer is troposphere that extends up to 10 or 11 km. This layer is the most dense layer and the temperature can fluctuate in between +17 to -52 degree celcius which comprises of almost all weather on earth. The temperature in this layer decreases as the height increases. After that comes stratosphere which extends up to 50km from tropopause where the temperature is increased with increase in height. This layer mostly absorbs the UV radiation, since ozone layer resides at this layer thus increasing the temperature of stratosphere. After this comes mesosphere which extends from 50 to 85km and is characterized by decrease in the temperature. It is even a place where the

coldest temperature in Earth's atmosphere exists which is near the poles. And then comes thermosphere where the temperature increases until it becomes constant.

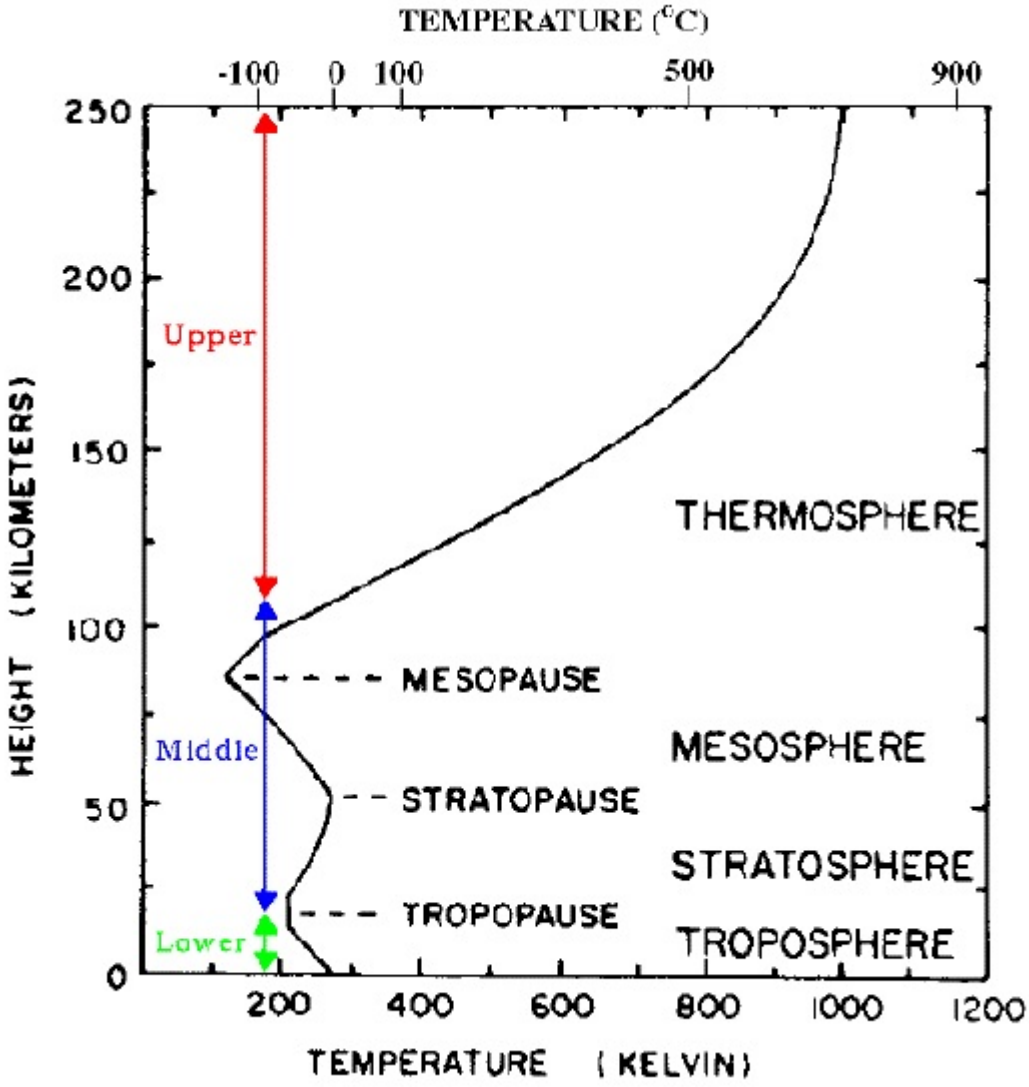

Figure 2.1: Temperature profile of the atmosphere

2.3 Temperature profiles in upper and lower mesosphere

The figure 2.1 shows the temperature variation according to the altitude. Here, what we can see is the minimum temperature exists near mesopause. One of the feature of mesopause is, it is more cooler in summer that at winter at poles.For instances, a mean temperature as low as 130K in the mesopause region during May- August

whereas, the temperature at winter is comparitively higher as 190 K(*Lubken and Von Zahn*,1991).

The normal direction of flow of zonal wind is easterly in summer hemisphere and westerly in winter hemisphere. As the warm air rises ,it moves to low pressure zone with expansion, thereby decreasing the temperature and thus causing the cold summer mesopause. The circulation of wind is considered as a result of gravity waves which comes in action because of the tropospheric winds. Now the question arises, how come such a low temperature in mesopause? The trend of flow is broken whenever the gravity waves reaches the stratosphere in summer, a special combination of eastward and westward winds in the stratosphere acts as a filter absorbing the zonal component of the wave more in one direction than in the other. Gravity waves continue with their upward propagation, and eventually, when they reach the mesosphere become unstable and break down, which entails an increase of momentum in one preferred direction in the mesosphere, which is able to change the summer zonal flow from easterly to westerly and also cause a meridional flow towards the winter hemisphere. The next event is flow of air travelling from the lower part of the atmosphere to the mesosphere, to keep the mass conserved. When this flow reaches mesosphere, it will cause an adiabatic expansion and cooling that results in lowering of the temperature in mesopause.[1]

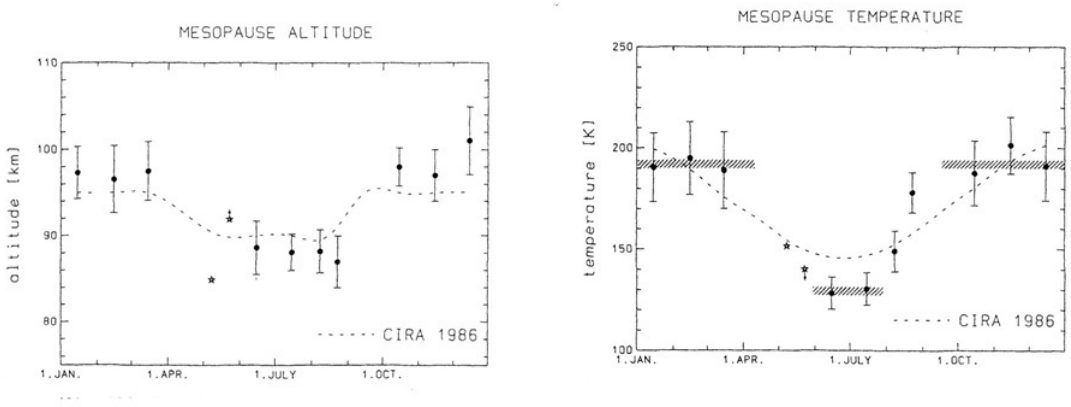

Figure 2.2: Temperature and height of mesopause as a function of seasonal variation(*Lubken and von Zahn, 1991*)

In addition, another explanation has been recently given for the cooling of the mesopause. Recently, it has been observed that unlike the troposphere, where the greenhouse gases results in the atmosphere heating up, increased CO_2 in the mesosphere acts to cool the atmosphere because of increased radiative emission by CO_2 which results in cooling of the mesosphere[2]. Further doubling of CO_2 concentration leads to an excessive cooling which can potentially leads to substantial changes in the structure and composition of the upper atmosphere. For example, these low temperatures during summer in the mesophere leads to the formation of ice particles with radius even larger than 20nm, which gives rise to another phenomena called as NLC.

2.4 Dynamics of mesosphere

To have a better understanding about the dynamics of mesosphere, we have to take under consideration the effects caused by atmospheric waves which are such as tides, planetary and gravity waves. Along with the observation of PMSE echoes, it has been observed that the variablity of the dynamics of mesosphere along with the temperature variations has helped in investigating the occurence of PMSE. Investigations of the mean winds, tides and gravity waves of the upper mesosphere and lower thermosphere region at poles have been studied with different radar techniques such as meteor radar, medium frequency (MF), mesosphere-stratosphere-troposphere (MST) and incoherent scatter radars.

2.5 Connections of PMSE

In mesosphere various chemical compositions play a vital role which are responsible for the dynamics of middle atmosphere. Though in recent times, many unexplained phenomenas have been explained, however there are still many phenomenas hiding beneath these layers undoubtly. Some of the phenomenas that have been revealed through continuous research is discussed below briefly in this section.

2.5.1 Noctulicent clouds

Often called as night clouds, these clouds are polar mesospheric clouds visible in summer times and at high altitudes. Characterized by multicolours with varying intensities of its constituent colours , the NLC are the highest clouds in the atmosphere which are usually found in the altitude range of 81- 85 Km where the temperature is around 140K[3], which is perhaps the mimimum temperature of earth's atmosphere. Because of such low temperature, macroscopic ice partilces exists in this regions which are believed to be associated with NLC clouds. The presence of these ice particles are believed to be the reason for the enhanced light scattering in the mesosphere(*Gadsden and Schroder*,1989). First observed NLC was reported by *Leslie* in 1885 [4].

Figure 2.3: Noctulicent clouds over night sky

Source: http://science.nasa.gov/science-news/science-at-nasa/2003/19feb$_n lc$/

The formation of NLC requires certain combinations such as low temperatures, water vapour and nuclei on which ice can grow. Unless the temperature is below 150K, ice cannot form at the low pressure. In addition, methane when reacts with hydroxyl radicals gives water which might be the source of water vapour in NLC. The methane is carried to this layer by the diffusion process [5].The terrestial activities have also been reported as a cause for such phenomenas. Volcanic and troposheric dust is another one of the possibility for the creation of NLC clouds but however, this is a rare case and was formulated on the basis of the first observation of NLC in 1884 shortly after Krakatoa eruption. The summer mesopause is getting even more colder due to increased concentrations of carbon dioxide and deposition of methane that have obviously linked to the change in global climate.

2.5.2 Geometry of NLC clouds

We can see the formation of NLC in northern hemisphere between the month of mid May and mid August. It can be seen from a latitudinal zone of 50-65 ^{0}N, whereas in the south between mid of November till mid February in the latitudinal zone of 50-65 ^{0}S.

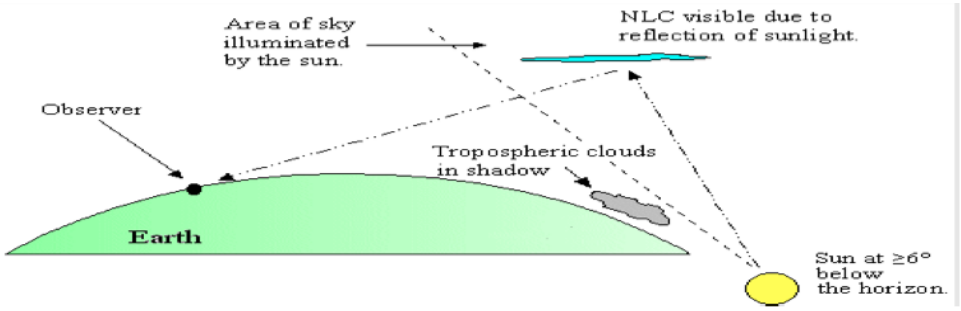

Figure 2.4: Geometry of NLC clouds

2.5.3 Gravity waves

The another influencing factor responsible for the dynamics of middle atmosphere is gravity waves. It plays a very vital role in energy transport and in the fluctuations of momentum in this region because of which the mean circulation and the thermal structure of mesosphere is affected to an extent. We can actually observe the gravity waves at different regions of atmosphere[6]. Some of the important factors that cause these waves are orographic forcing(*Smith,1979,1989; Queney,1948; Rottger,2000*),deep convection (*Nastrom et al., 1990*), the interactions between wave to wave (*Ruster,1994b*), frontal activity (*Schollhammer,2002*) and thunderstorms (*Chimonas and Nappo; Finke,1995*).

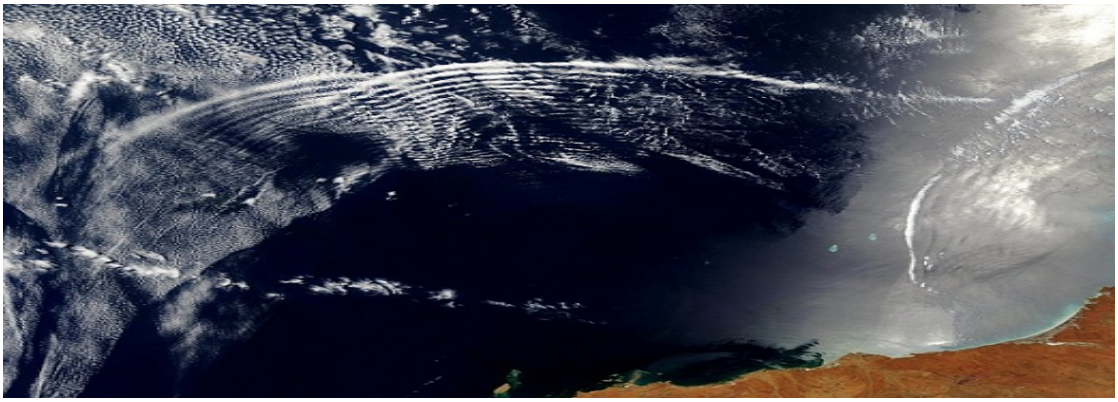

Figure 2.5: A glimpse of gravity waves

Source: http://weatherwars.info/tag/gravity-waves/

In summer time, the gravity waves reaches the mesosphere because of very strong filtering process in the stratosphere. As it reaches in high altitudes where the density is lower, its amplitude increases so as to keep the energy conserved and finally becomes unstable and it breaks down, thus creating the difference in pressure causing the change of normal flow of zonal winds in the reverse direction. Not only that, this effect causes the vertical up flow of air in high latitudes. This lifted air in the mesosphere expands adiabatically and thus causes cooling.[7]

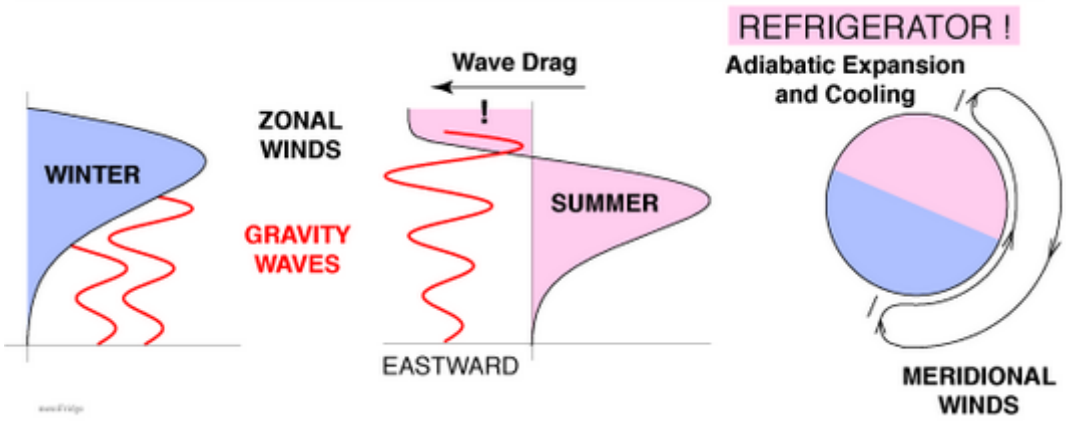

Figure 2.6: Figure to show the cooling of mesosphere with aid of gravity waves

Source: http://tupac.phys.uit.no/ cesar/MORROradarSite/accordion/SpryAccordion.html

2.5.4 Charged aerosols

The investigation shows that the presence of charged aerosols accounts for the scattering process and if these aerosols are charged at an optmized condition can be responsible

for a high radar reflectivity at UHF and VHF radar[8].The study and investigations had shown that the presence of negative charges on the ice particles which are associated with the thermal currents. The thermal current because of electrons is higher to that of ions because of higher flux of electrons in to the ice particles[9]. And this higher flux of electrons to an ice particles is because of higher velocity of electrons than ions. Further, the size of these particles also plays a role in directing the intensity of PMSE power. The modeling of such aerosols shows that the diffusivity reduction is proportional to the square of the radius only if a required amount of charge is present on the aerosols such that N_A Z_A / $n_e > 1.2$ (where N_A = number of aerosols,Z_A= aerosols charge, n_e= number of free electrons)[10]. More explanations is made in chapter 3 under section 3.5 about the charging of ice particles.

Chapter 3

Polar mesosphere summer echoes

3.1 Introduction

Since a long time many efforts have been put forward to unreveal the hidden truths of the atmosphere. The atmosphere has prove itself as a platform for different researchers and scientists to let them know the hidden secrets unfolding itself. Various environmental issues are directly related with the phenomenas occuring in the atmosphere. In recent times, the increased number of population had shown a tremendous effect on the existing environment in one way or the other. For instances, the man made pollution might change the dynamics of the atmosphere till hundreds kilometers of heights and therefore these changes in higher layers might affect the lives on Earth indeed. Here we are mainly focussed in polar mesospheric latitudes and the interesting phenomena called Polar Mesosphere Summer Echoes(PMSE). In addition to this, other phenomena such as Noctulicent clouds(NLC), gravity waves and charged aerosols are generally found associated with PMSE which were briefly discussed in second chapter.

3.2 Definition

Polar mesosphere summer echoes (PMSE) are basically strong radar echoes that are observed at an altitude of 80 - 90 km by very high frequency (VHF) radars. These phenomena were first observed in 1979 with 50 MHz radar at Poker Flat at 65^oN, Alaska by Ecklund and Balsey. Later on in mid-latitudes, summer echoes were again observed by 53.5 MHz radars in Germany(*Czechowsky et al.,1979*) which were proposed to be of another nature and characteristics than those observed at high altitudes, and since then various researchers and scientists have been indulged in this area to unfold the hidden secrets behind PMSE[11]. The name PMSE simply comes from the fact that these echoes are summer time echoes in the mesosphere regions reaching almost a maximum SNR of about 30dB. Generally these echoes are found in so called mesopause regions and

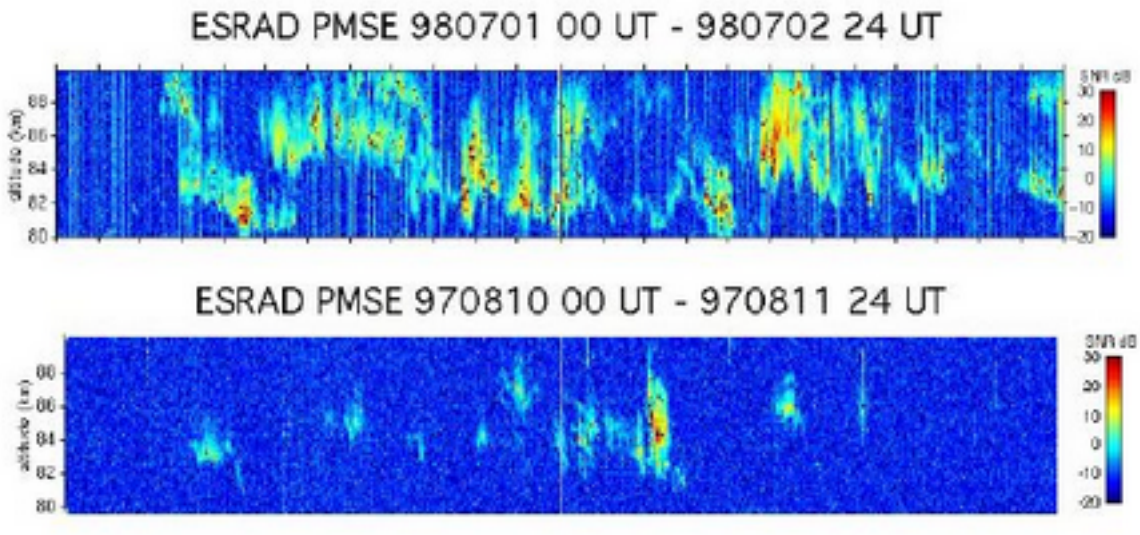

Figure 3.1: PMSE variations at different altitude against universal time

Source: http://www.irf.se/program/afp/nlc/

are characterized by very low temperatures almost down to 140 K in the summer and around 190 K in winter above the poles[12]. The seasonal variation, seasonal occurence of PMSE, observational frequencies in these echoes will be discussed briefly in this chapter.

3.3 Occurence

Along with the studies of these echoes, it was found that these echoes were abundant in polar regions at high latitudes during summer . The observation shows an increase in occurence at end of May and a slow decrease in mid of August(*Balsley et al., 1983; Kirkwood et al., 1998*). To an extent, this variability of occurence of PMSE can be explained on the basis of temperature fluctuations. The fine combination of temperature and presence of optimized water vapour plays the role in forming ice aerosols, which according to late research suggests association with formation of PMSE. Furthermore, the degree of saturation S which is the ratio between the partial pressure of water vapour P_{H2O} and the saturation pressure of water vapour over ice is P_{sat} is more than 1, the particles can exist or can grow, for the value less than 1, it will evaporate. According to Marti and Manersberger(1993), the value for P_{sat} can be given as,

$\log_{10} P_{sat} = 12.537 - 2663.5/ T$ [13]

In accordance with the equation given above, we can say that in the early summer around early May, very less temperature is needed to form the ice aerosols. Existence of such aerosols is associated with PMSE occurence.

Furthermore, the occurence of PMSE varies in different times within a day, basically called as diurnal variations. It has been shown that occurence is minimum at 20:00 LT(Local time) and maximum after 12:00 LT (*Balsley et al., 1983; Hoffmann et al., 1999*)[14].

3.4 Observation of PMSE

Since the PMSE were started to be studied, these were observed in different frequency range. For instance, it has been observed in range from 2.78 MHz (*Bremer et al., 1996*) and 8-9 MHz (*Karashtin et al., 1996*) to 224 MHz (*Hoppe et al., 1998; Rottger et al., 1988; La hoz et al., 1990*) and 933 MHz(*Rottger et al., 1990*) and at 50MHz . And PMSE are generally observed at latitudes above 60 N, whereas sometimes they have been even encountered as far as south as 52 N in Harz mountain(Germany) with 53.5MHz SOUSY radar(*Czechowsky et al., 1979*) and 52.4 N in Aberystwyth, Wales by 46.5 MHz radar (*Thomas and Astin,1994*).

3.5 Factors affecting on PMSE

Recently, it has been discovered that the presence of such enhanced echoes in upper atmosphere is because of the turbulence aided by enhanced Schmidt number in the presence of the charged ice particles.

- Turbulence

  The measurements were made to see the correlation between turbulence and presence of PMSE. Direct measurements from Lübken et al.[1993] shows that the occurrence rates for PMSE and neutral air turbulence were at same heights. The turbulence though is present in all altitudes,but at heights around mesopause , the turbulence rate is higher which can conclude that neutral air turbulence is factor causing PMSE. The figure here shows the variation of turbulence along different heights being higher around 87Km.[15][16]

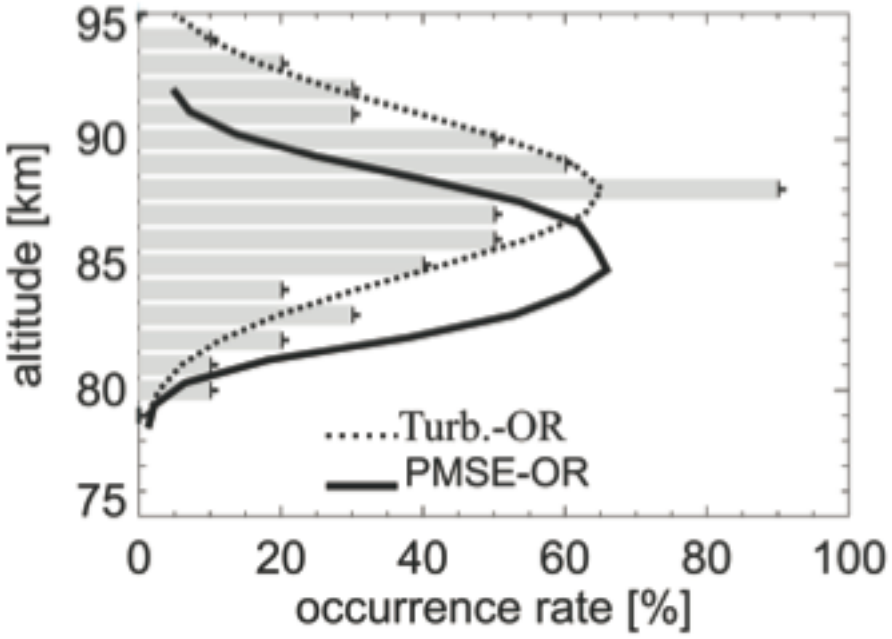

Figure 3.2: The ocurence rates of PMSE(solid line) and neutral air turbulence(dashed line),*Rapp and Lubken*[2003]

- Ice particles

  The diffusion of methane in atmosphere which reaches mesosphere produce water from chemical reaction. These water because of very low temperature gets converted to ice. From the study, it has been known that the NLC clouds occurring in the heights of around 80- 85 km is due to the ice particles. Again, what it has been shown is , the occurrence of NLC and PMSE have same seasonal variations. This can conclude that the presence of ice particles is one of the reason to produce NLC clouds and presence of NLC clouds shows the presence of PMSE echoes. The ice particles which has their radius in between 10 to 15nm and has tendency to capture electrons and become negatively charged. Due to the higher flux of thermal electron to the ice particles compared to ions, it can be embedded higher in the ice particles thus making it negatively charged. The ice particle continue charging negatively until and unless the current due to negative charge and positive charge are equal and opposite to each other the making the total thermal current zero. Thereafter, it reaches to a steady state where it can neither take nor give electrons[10].

- Electron density

  The presence of electrons is the most important factor leading to PMSE. It is known that the backscatter of the radio waves is because of the irregularities in density of

electrons. So, presence of sufficient electron is required to cause PMSE. The PMSE has a wide range of electron densities between 300/ cm^3 and $10^5/cm^3$.The factor that can bring a change in the electron density can play a role in influencing PMSE. For example, the electron diffusivity is increased during heating thus destroying the irregularrities in electron density and thus producing weaker PMSE.[17]

3.6 Properties of PMSE

3.6.1 Dependence on Radar frequency

Since the beginning of observation of PMSE , it has been observed that the PMSE has its dependency on the frequency of radar. The occurence of PMSE has its range from frequencies in between 2.78MHz to 1.29GHz. The table below shows some results including the reported absolute volume reflectivities.

Frequencies(Braggs scale)(MHz)(m)	Location	Reference	Reflectivity (m^{-1})
2.78(53.9)	Tromso	Bremer et al(1996)	
8-9(18.8)	Vasil'surk ,Russia	Karashtin et al.(1997)	
49.6(3.0)	Tromso	Rottger et al.(1990)	$2.0.\ 10^{-12}$
50.0(3.0)	Poker flat	Ecklund and Balsley (1981)	$9.0.10^{-15}$
51.5(2.9)	Resolute Bay	Huaman et al.(2001)	
53.5(2.8)	Andoya	Inhester et al.(1990)	$4.0.10^{-12}$
224(0.67)	Tromso	Rottger et al.(1988)	$1.5.10^{-16}$
500(0.3)	Svalbard	Rottger(2001)	$5.3.10^{-19}$
933(0.16)	Tromso	Rottger et al.(1990)	$1.2.10^{-18}$
1290(0.12)	Sondrestrom	Cho and Kelly (1992)	

Figure 3.3: PMSE studies at different frequencies

The interesting thing that we can see from the table is that the the volume reflectivity shows a tremendous decrease with increase in frequency (decreasing Bragg scale).

3.6.2 Spectral shape

The information encoded in the spectral shape is one of the important properties of PMSE. From the explanation in Hocking (1989), the doppler spectral width gives the information on the velocity variance of the detected scatterers in the radial direction (= in the pointing direction of the radar beam). The spectra obtained from the PMSe

have a gaussian shape most of the times. Because of turbulence associated , the spectral width changes. On the basis of spectral width, one can know the nature of turbulence prevalent in such echoes. For example, higher turbulence creates higher velocity variance and hence wider spectral width and vice-versa.

3.7 Seasonal variation

The variation of PMSE is characterized by the increament by the end of may, high in the month of june and july and gradual decrease during august. This is because of the role played by temperature which is low in the month of june and july in the mesosphere.

Chapter 4

Theory on PMSE and objective of the thesis

4.1 Overview

Since the beginning of observations made for PMSE, different experimental methods are implemented to find out the physical process lying beneath this phenomena with high accuracy. From the research, it has been shown that, the irregularities in the electron density cause the back scattering of the radio waves, thus generating echo. Generally there are two kind of scattering mechanisms that occur from the high atmosphere. They are incoherent scatter and the other is coherent scatter. The incoherent scattering comes from the random fluctuations of electrons under thermal equilibrium. Other than that is coherent scattering which one of its form is PMSE as in our case and which are very strong backscattered echoes in compared to incoherent scattered echoes.

4.2 An explanation on its origin

Many methods were implemented to know the physical process lying behind this phenomena. The main reasons are mesospheric turbulence and charged ice particles that generates such enhanced echoes. It was propsed by *Kelly et al.*[1987] and *Cho et al.*[1992] that the ions and charged ice particles results in reducing electron diffusivity because of ambipolar forces. Overall, the main factor determining the echo power received is because of turbulence and high Schmidt number [18] [19].

Characterized by random and stochastic process, rapid variation of velocity and pressure is turbulence(Wikipedia). The theory of turbulence shows the transfer of energy from larger eddies in to smaller eddies . The larger eddies which are unstable breaks down in smaller ones and this breaking up process continues until the Reynolds number becomes

too small at Kolmogorov scale(K) that the molecular viscosity comes in to play dissipating the kinetic energy and thereby coverting the dissipated energy in to heat and at these K scales, there are no any irregularities left to cause scattering[18].

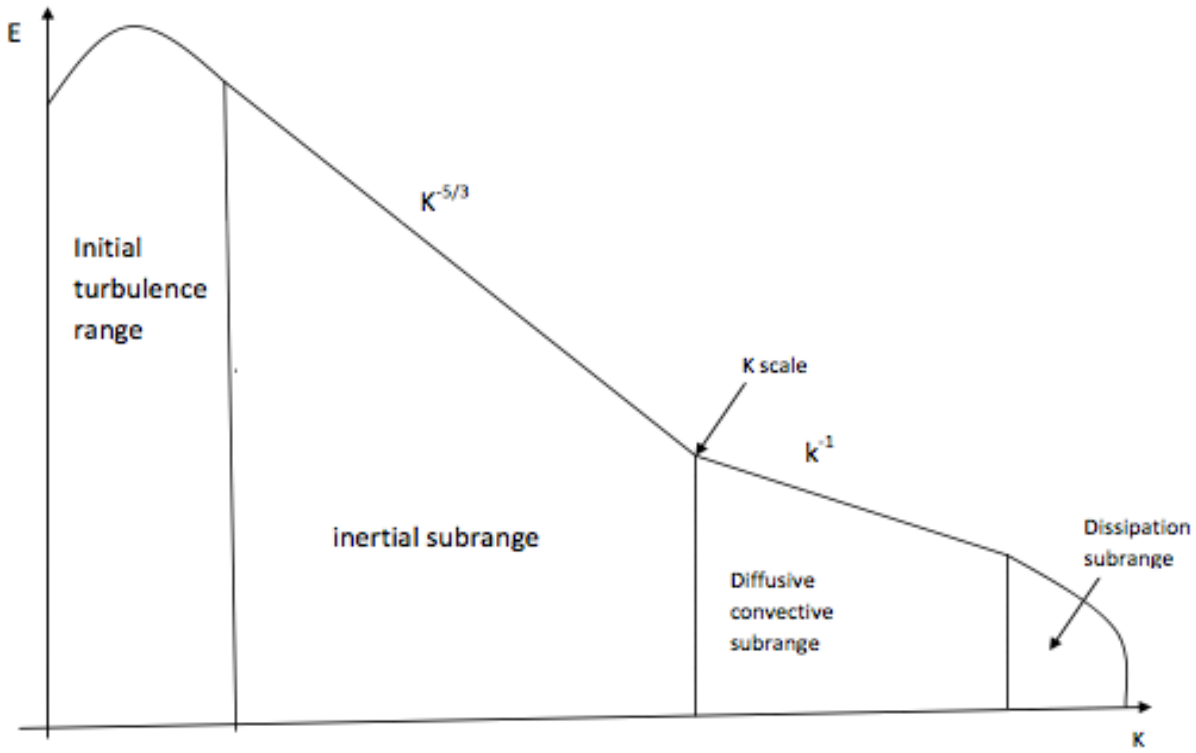

Figure 4.1: Kolmogorov spectrum

The breaking of larger eddies in to smaller ones occurs in the inertial subrange region represented by the flat zone with dependence of $k^{-5/3}$ as we can see in the figure 4.1. When the eddies reaches the K scale(the point beyond which the irregularrities do not exists), it dissipates in the region called as dissipation range.The VHF and UHF radar have their K values beyond the K scale.However, we can still see the irregularities beyond this K scale which is explained by the help of extended kolomogorov density spectra with enhancement of Schmidt number [15] .

A mathematical model has been introduced to represent the electron diffusivity and kinematic viscosity of air to look at the relation with Schmidt number that can say something about the cause of PMSE.The Schmidt number Sc is given as the ratio of kinematic viscosity of air and electron diffusivity as υ/D. When Sc is much larger than 1 , which suggests, the electron diffusivity is smaller in comparision to the neutral air kinematic viscosity, then the density spectra extends over to the diffusive convective subrange which is characterized by k^{-1}dependence[*Batchelor*,1959] as shown in figure

4.1. This is caused due to the presence of charged ice particles where the ambipolar force holds the electrons in the place around the ice and decreases the electron diffusivity rate which suggests that the electron density fluctuations driven by neutral air turbulence can have a chance to exist in smaller scales that can give scattering in VHF and if the irregularities exists even in much smaller scales, scattering can be seen in UHF radar too[20].

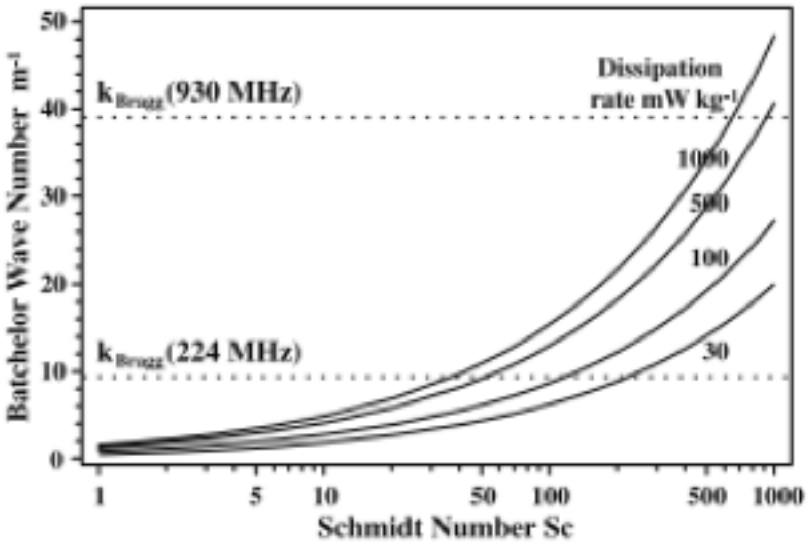

Figure 4.2: Batchelor wave number as a function of Schmidt number, *C.La Hoz et al., 2006*

From the figure 4.2, it can be shown that with Schmidt number around 50 and 200 can give rise to PMSE at VHF Bragg wavelength 67 cm with energy dissipation rates between 500 and 30mW/kg respectively. So, theory given by enhanced Schmidt number is vey useful in explaining the existence of PMSE even in such low dissipation rates [21].

So, we can summarize ourselves that there are two factors, i.e., charged ice particles and the neutral air turbulence with enhanced Schmidt number that plays an important role in PMSE formation at VHF and UHF Bragg wavelength.

4.3 Objective

The thesis is not actually arguing with any of the facts explained, however it tries to see the effect of turbulence on the spectral width as a function of time and height. In addition to this, the change in the dissipation energy rate in PMSE with varying spectral width is

shown. The major objective of this thesis is designed to understand the phenomena and relate with different factors, which for instance is turbulence in my case. The findings on power of PMSE and the variation of doppler velocity of PMSE is also under target to have a more better feeling about the statistical properties of PMSE.

Chapter 5

Radar Techniques and processing

5.1 Introduction

The radar observations have filled up a huge gap in understanding the upper atmosphere and its dynamical characteristics. Even a small change in the atmosphere can be detected by these radar technologies. For instance, a change in wind, waves and turbulence that plays an important role in changing the dynamics of the atmosphere can be detected by these radars. A complete knowledge of climatic changes needs comprehensive study of the dynamics of the atmosphere mainly between the region of troposphere and 100km height.Generally, when a wave is allowed to propagate undisturbed in its medium , it can go a long way without being reflected or scattered. However, due to the radiowave scattered by the turbulence or by radio refractive index (RRI) perturbations caused by the turbulence(of the order of half the radar wavelength) produce such echoes. High up in the mesosphere, the main cause for such perturbation in RRI is the fluctuations in the electron density(Tatarskii, 1961). In this chapter, the contents will be mainly focussed on the radar principles, its observation methods, scattering mechanisms.

5.2 Scattering

On our general understanding, we have learnt that the scattering is a physical phenomena in which the radiation are deviated from its trajectory which might be due to the presence of non-uniformities in the environment. Scattering of radio waves transmitted from radar is important phenomena and one of its basic example is incoherent and coherent scattering.

- Incoherent scattering

  The scattering of electromagnetic waves from the thermal random fluctuations in electron density under thermal equilibrium is called Incoherent scattering. The

basic idea of incoherent scattering comes from Thomson scattering, i.e., scattering of the electromagnetic waves by free electrons.From those reflected back echo, one can measure the parameters like electron density, wind temperature, composition and velocity of electrons by the use of incoherent scatter radar systems which is the effective groundbased technique that has been in use since a long time to study the earth's ionosphere and its interactions with the upper atmosphere.The Incoherent scatter(IS) radar, allows us to study the atmosphere from height ranging from about 60 km to thousands of kilometers.

- Cohorent scattering

  In the absence of thermal equilibrium , there can exists high electron density fluctuations which might be because of high turbulence and plasma instabilities than can gives higher scattering and hence more enhanced echoes called as coherent scattering and one of its kind is PMSE.

5.3 EISCAT

It is a scientific association for international research which till date is operating three incoherent scatter radar systems at 931 MHz,224MHz and 500MHz in Northern Scandinavia. EISCAT (European Incoherent Scatter) uses incoherent scattering mechanisms to study the upper atmosphere which transmits a highly powerful electromagnetic waves which are scattered from the irregularities and are received back for analysing. One of the important work carried out is by VHF radar studying the mesosphere and phenomenas like PMSE. Figure below shows the installed radars facility which consists of UHF radar for study of ionospheric activities and VHF radar which extends its range of use in science that are operated by EISCAT. Here in Tromso, we have VHF(224MHz) corresponding to Bragg wavelength 67cm and the other UHF (930MHz) corresponding to Bragg wavelength 16cm. Remote sites for UHF are located in Sweden and Finland and there is a small array called as EISCAT-3D demonstrator in Kiruna that receives for Tromso VHF radar and from this I get my data for analysis.

The EISCAT UHF operates at a transmission power of 2MW. The antenna is a 32 metro diameter disk that weighs around 100 tones. It can be steered fully. The next is VHF operating at 1.5 MW peak power[**?**].

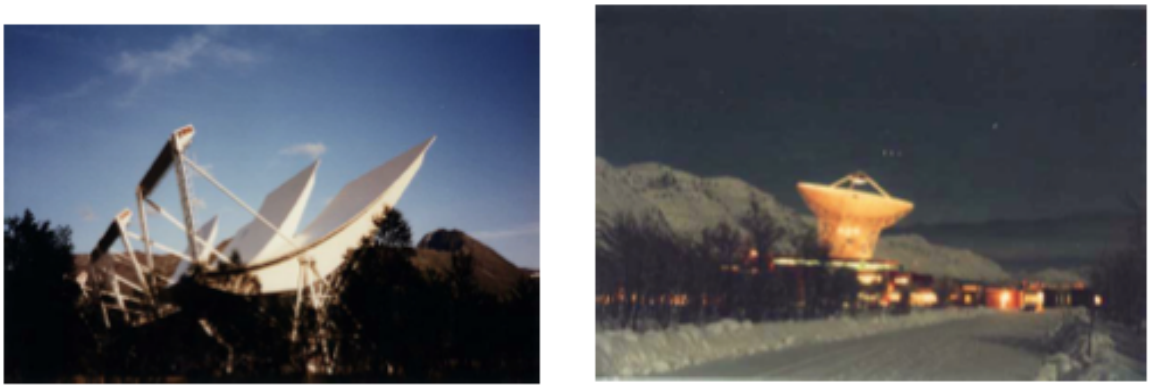

Figure 5.1: Left panel shows VHF radar and right panel sows UHF radar in Tromso.

The other one is EISCAT 3-D demonstrator which contains a phased array of 48 Yagi antennas(antennas consisting of a driven element typically a dipole or folded dipole) and is capable of detecting the signals from VHF Tromso. The data obtained for thesis is from this radar shown in figure 5.2

Figure 5.2: EISCAT 3-D demostrator, Kiruna

The geographical location of the EISCAT radar is shown by the figure 5.3 followed by a

table showing the values of some radar parameters.

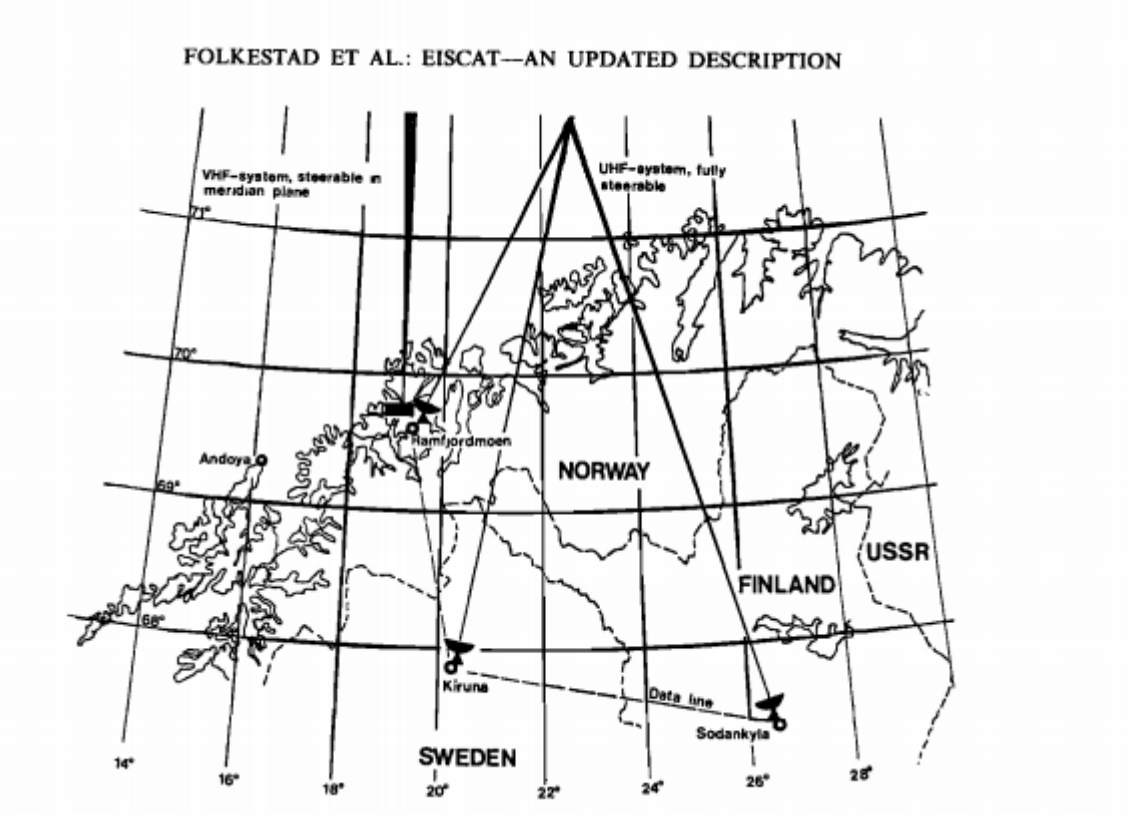

Figure 5.3: Installation of EISCAT radars

- Radar parameters of EISCAT radars

Table 5.1: Radar parameters

Parameters	EISCAT VHF	EISCAT UHF
frequency(MHz)	224	930
wavelength(m)	1.34	0.32
Bragg wavelength (m)	0.67	0.16
System Temperature(K)	250-350	110
Peak Power(MW)	1.5	2

Chapter 6

Methodology and procedures used in the Analysis

6.1 Overview of the process

In this chapter the process and the procedures used in the signal analysis of the data obtained will be discussed. The experimental data is originated from the enhanced radar echoes from the polar mesosphere observed from EISCAT. The data obtained is from EISCAT 3-D demonstrator antenna array receiving signals from VHF transmitter from Tromso from year 2011 July.

The calculation of the spectral width of spectrum from such echoes shows the presence of turbulence and is proportional to the intensity of the measured turbulence which is mathematically expressed in terms of the turbulent dissipation rate which is measured in the unit miliwatts per kilogram. Before going on the procedures that i had implemented in the statistical analysis, its worth describing some parameters associated with it.

6.1.1 Parameters

We have autocorrelation function from which we obtain spectrum using Wiener khinchin relation. It was seen that the frequency power spectrum so calculated had a gaussian shape because of which gaussian fitting was made to the spectrum. From the fitted gaussian model, the parameters like amplitude, doppler shift and spectral width were calculated which are described below here briefly.

The gaussian model use to fit the spectra in my case is

g[x] = A $\exp^{-(x-d)^2/(2*\sigma^2)}$,

where g[x]=gaussian function,A= amplitude, d= doppler shift and σ= spectral width.

- Amplitude

  The peak value of the spectrum is termed as amplitude(A).

- Spectral width

  The width(σ) of the spectrum is a measure of the dispersion of velocity. It tells us about the variability of the radial velocity because of factors like wind shear and turbulence. The width measured here is in hertz which is converted to m/s for further calculation of dissipation energy rate to see the footprints of turbulence in PMSE echoes.

- Doppler shift

  It is the change in the frequency of a wave that occurs due to the relative motion between the observer and the source. The value of "d" gives the doppler shift in hertz which can be changed to the doppler velocity from relation

  $V_d = \lambda_{radar} * f$d/2, where

  λ_{radar} =wavelength of radar, f_d = doppler frequency, V_d = doppler velocity

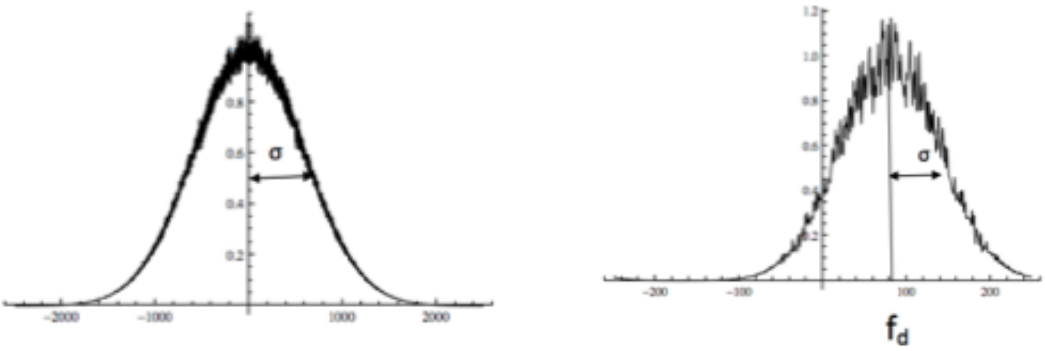

Figure 6.1: Figure showing the spectra with zero doppler shift and doppler shifted

- Dissipation rate

  The important feature of turbulence is that it is dissipative.The rate at which the turbulent energy gets dissipated per unit mass is called as Dissipation rate. For our case, it is given as

  $\epsilon = 8.4 * \sigma^2$,where σ is the spectral width in m/s.[20]

  Calculation of ϵ can tell us about the variation of dissipation at mesosphere as we will see in the results.

6.2 Methodology

In this section the methods which has been implemented in the data analysis in this thesis will be discussed. For this ,I had used Fourier Transform and and spectral fitting.

X(f) = F$x(t)$ = $\int x(t)\mathrm{e}^{-j2\pi ft}$ dt

and

x(t) = F^{-1} X(f) =$\int X(f).\mathrm{e}^{j2\pi ft}df$

where,

F$x(t)$ = Fourier transform of x(t)

x(t) = signal in the time domain

X(f)=complex signal in the frequency domain.

Based on the theorem proposed by **Wiener khinchin** , we have a relation between power spectral density and autocorrelation function which is given as ,

S(f) = $\int R_{xx}\exp^{-i(2\pi * f * \tau)}\,d\tau$

where, $R_{xx}$is the autocorrelation function,

f is the frequency,

τ is time

Finding the Fourier of the ACF will be continued by fitting the obtained spectrum to a gaussian model. Fitting a data set to a model function gives us the best fit parameters. After finding the associated parameters to the spectra, further analysis was carried out such as finding dissipation rate, doppler velocity and power of the signals.

Examples of plot done from mathematica is shown below. The figure shows the plot of ACF for a particular gate at gate number 17(83.34km) and time at 10:46am. The spectrum calculated here as we can see is of gaussian shape. The fitting done to this particular spectra is also shown here. The fitting was repeated to all of the spectra in all time and heights.

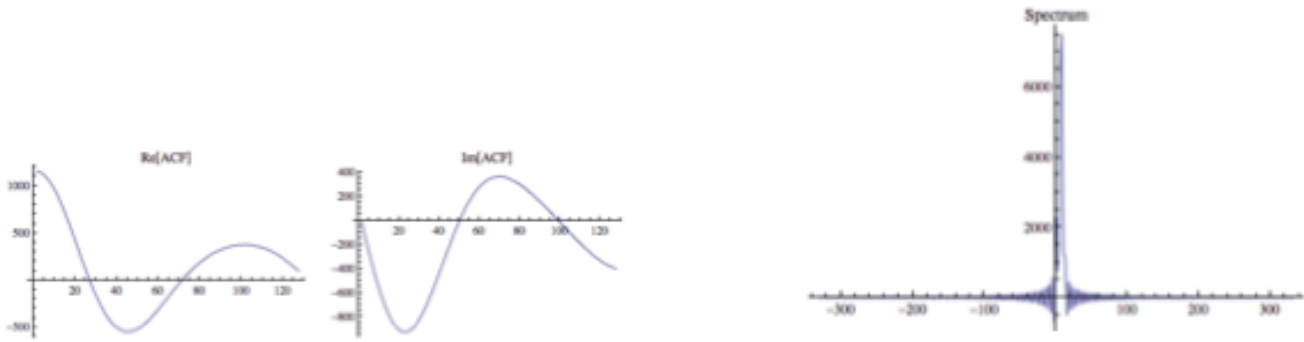

Figure 6.2: Figure showing the ACF and its spectrum

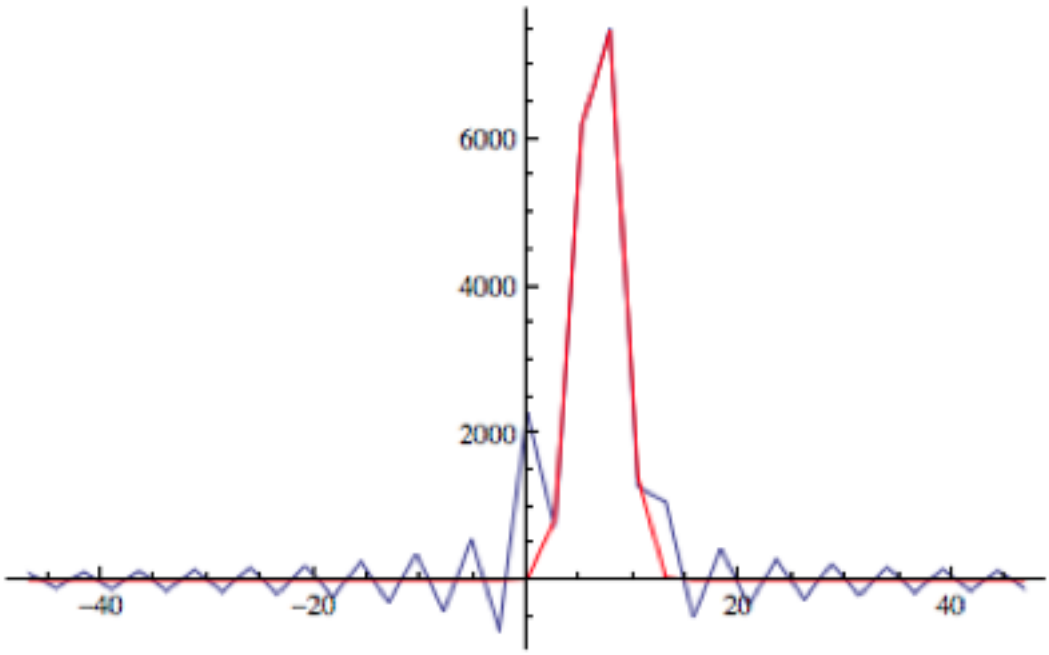

Figure 6.3: Spectrum fitted to gaussian. Red line is the fitted one

6.3 Data Simulation

The data simulation begins with the design of a linear filter which can be represented as

$Y(\omega) = H(\omega)X(\omega)$,

where

$Y(\omega)$ =output spectrum

$H(\omega)$ =Transfer function

$X(\omega)$ = White noise spectrum with a constant value.

We now take a white noise x[n] which have gaussian distribution as an input to a system with h[n] as impulse response and y[n] as output as shown in the figure 6.4.

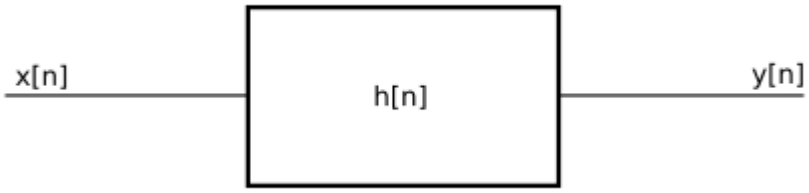

Figure 6.4: Block diagram to show the input and output convolved with impulse response

From the relation $Y(\omega) = H(\omega)X(\omega)$, we can have a relation between $Y(\omega)$ and $H(\omega)$ since $X(\omega)$ is now constant. So,

$Y(\omega) = H(\omega)$[considering $X(\omega) = 1$, for ease]

Now, to calculate $H(\omega)$ with power spectrum $S_Y(\omega)$, we have a relation,

$H(\omega) = \sqrt{S_Y(\omega)}, (since Y(\omega) = H(\omega))$

from which the impulse response h[n] can be calculated as the inverse fourier transform of $H(\omega)$.The output signal can be found out by convolving the impulse response with white noise.

$y[n] = \sum_{k=-\infty}^{\infty} h[\tau]x[n-\tau]$

Taking the square of absolute of fourier transform of output signal, we can finally obtain the spectrum which has a gaussian nature.This is random in nature and to make it more smooth, I had averaged it in many realizations of random signals. And after that , the simulated output spectrum is fitted with a gaussians model to find its parameters.

Fitting is a process of capturing the trend in the data by assigning the standard functions along the entire range of the data. This gives us the best fit parameters to a set of data. Looking at the plots in right panel in figure 6.5, it can be known that the spectra has a gaussian shape and hence to know the parameters associated with it , the gaussian fitting is used. The parameters like amplitude,doppler shift and the width is found for the spectrum. The spectrum that I started was with zero doppler shift. However, to have a doppler shift, the time series of the output signal can be multiplied with $\exp(-j2\pi f_d t)$,

where f_d is the doppler shifted frequency. In addition, the time series of zero doppler shifted spectra has real values whereas the doppler shifted spectra has complex values in time series. Hence, even looking at the time series, we can know if the spectrum is doppler shifted or not.

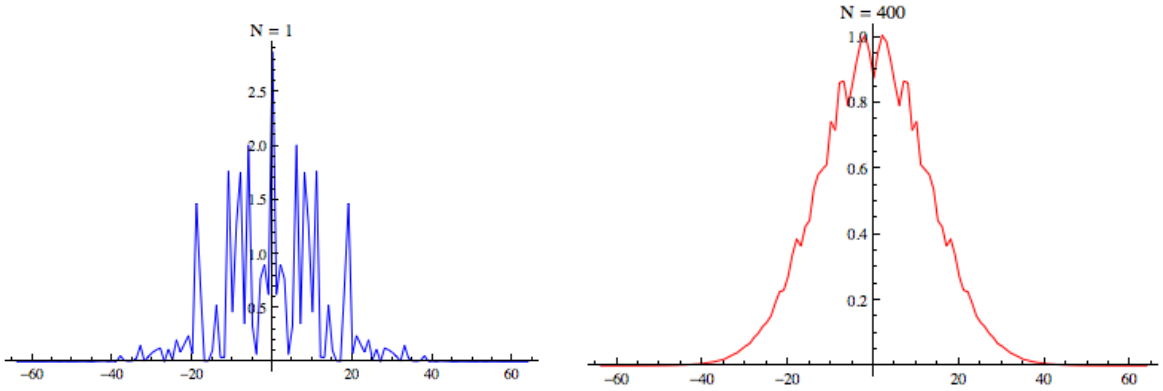

Figure 6.5: Left showing the noisy spectra and right showing the averaged output spectra with zero doppler shift

The figure 6.6 shows the fitting to the spectra. The purpose to start with synthetic data simulation was to develop an idea about processing the real data obtained for thesis.

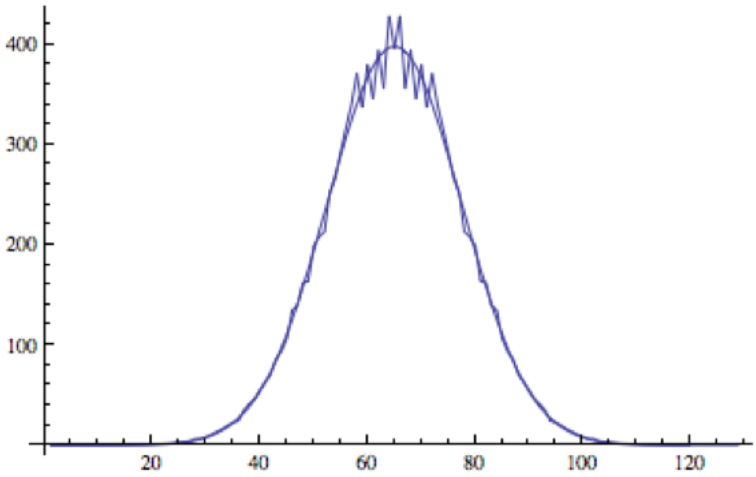

Figure 6.6: Gaussian fitted spectra

6.4 Data analysis

The Data structure of the EISCAT is a root directory which contains one hour directories which contains a number of data files. Here , first a flat list of data files corresponding to one- hour is made. The ACF measured was with the 127 points from lag 1 to 127 with zero lag missing. The data was extracted from VHF radar Kiruna on 2011 july 11 from time approximately 10:38 till 12:15 in the day time. The first step was to make zero lag ACF. For this, the first two consecutive lag from the positive time delay as shown in figure was reversed and the curve was extra plotted in negative time. This procedure makes the ACF zero lag and to make it symmetrical all the remaining points in positive delay were reversed in negative time to make ACF symmetrical with length of 128 in positive time, 127 in negative time and including zero which now makes ACF a total of length of 256.

After this, the Fourier transform was used to find the spectra and gaussian fitting was made. Fitted models for all the spectra was found and the parameters like amplitude, doppler shift and width were calculated. From the calculation of doppler shift, I calculated doppler frequency and from which I calculated doppler velocity in m/s. From width(in m/s) I was able to calculate the Energy dissipation rates. Doppler velocity (radial velocity) was calculated from the formula given as , doppler velocity V_d = fd$*\lambda_{radar}/2$, where λ_{radar} is the radar wavelength which is 1.34 m in our case. Further to calculate the Energy dissipate rate, I used Energy dissipation rate $\epsilon = 8.4 * \sigma^2$where σ is the width. in m/s and ϵ is in mW/kg.

Chapter 7

Results

7.1 Overview

From the data analysis of PMSE, some of its statistical properties were extracted out as results which will be discussed in this chapter. Here I have made the measurements of width, amplitude, power and doppler shift of PMSE on July 2011. In this chapter , the results of such parameters at different time will be shown and possible explanations will be given. The results will be mainly concentrated finding the spectral width and Energy dissipation rates with possible explanations of footprints of turbulence in it at different heights at respective time. Before that, ACF and its shape will be discussed followed by the calculation of power, width, doppler and dissipation rate.

7.2 Autocorrelation of obtained PMSE

To start the result , its worth showing the autocorrelation functions obtained from the data. Starting from the first gate till 53rd at time 10:46:48 with a sampling rate of 1.5 ms, the figure is shown below. The ACF shown in figure 7.1 is with a missing zero-lag which was later on corrected with extra plotting and making the ACF symmetric as mentioned in section 6.4 in data analysis. The figure clearly shows that we have signals at only few gates. Most of the gates contains contains no signal (means no irregularities). So, the echoes cannot be seen compared to the irregularities in gates 14-23 as we can see in figure 7.1.

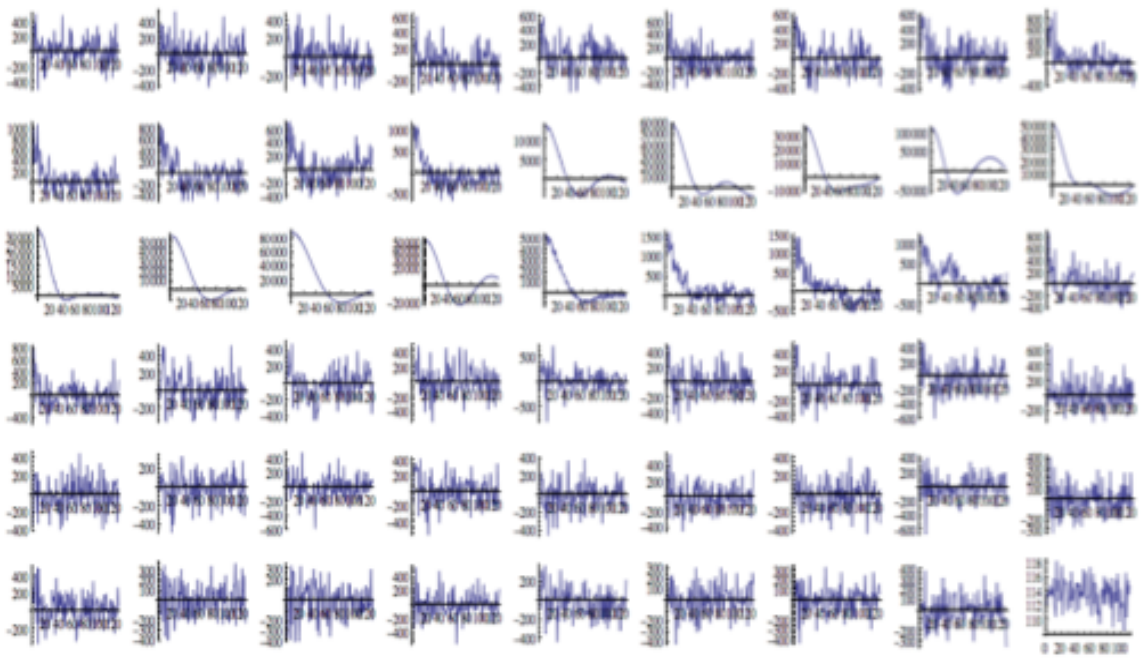

Figure 7.1: Showing the ACF with total gates 53 at time corresponding to appx 10.46 am on 11th July 2011..

To look at it more precisely and compare the plot of ACF at 3 different gates at the same time were plotted to have a feeling of comparison to other ACF at different gates.

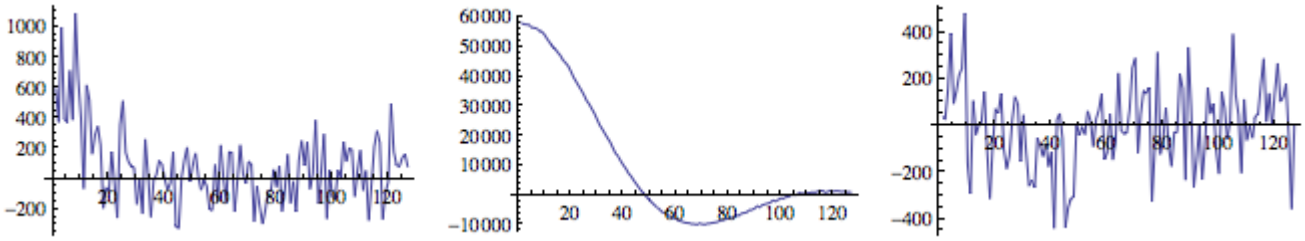

Figure 7.2: ACF at gate number 10, 20 and 30 respectively at time appx 10.46 am on 11th July, 2011

7.3 Power of PMSE

The power of PMSE vary as a function of time and height. It was found that the signal could be measured only at few gates where the irregularities are sufficient to produce

density fluctuations as shown in figure 7.3 and 7.4. These plots are made after subtracting the noise from the signal.

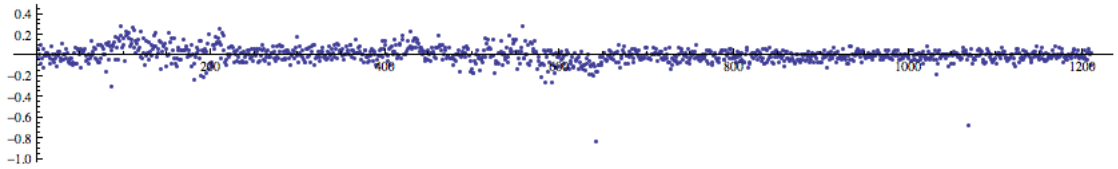

Figure 7.3: Variations of power at gate number 43

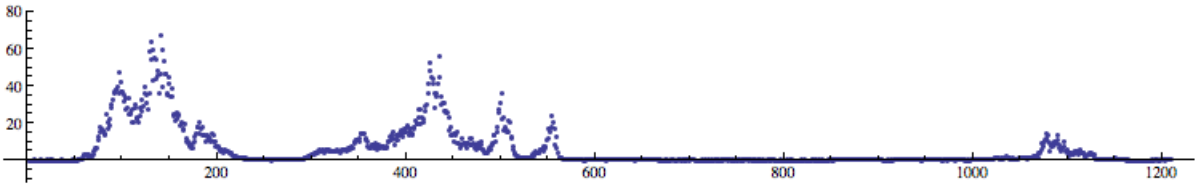

Figure 7.4: Variation of power at gate number 15

Comparing these two figures, it can be seen that the power at gate 43 fluctuates in between +0.2 and -0.2 (approximately) which is actually the residual fluctuations around zero, whereas the power at gate number 15 has peak value of almost more than 60 which suggests the presence of signals where the values is positive and becomes larger than at gate 43. Combining all the power values in total time along total heights as obtained is shown below.

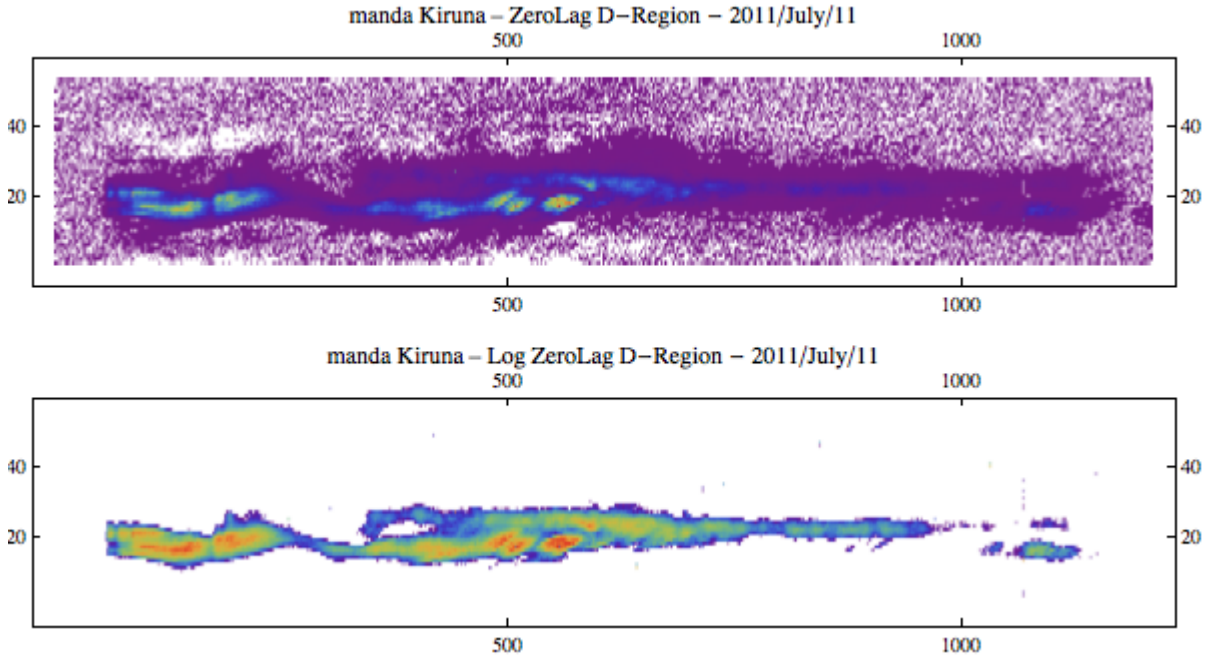

Figure 7.5: Power of PMSE

A more detailed and clear figure was obtained using a combination of Java to make the plots of power variations. The time resolution made was 4.8 second and the height resolution was 0.7km

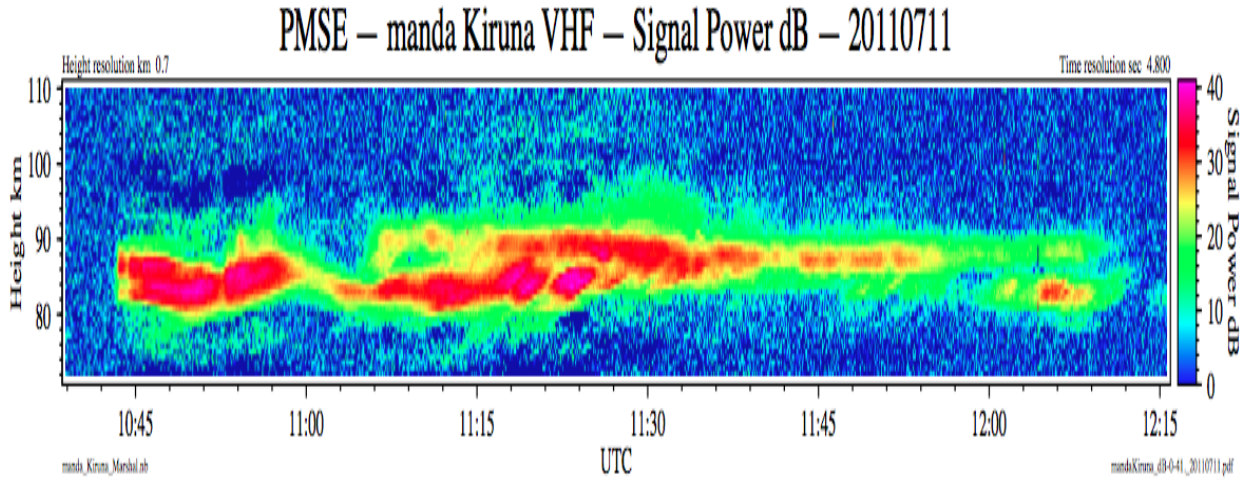

Figure 7.6: Power variations of PMSE in Year 2011 july 11 between time 10:38 to 12:15 in day

From the figure 7.6, it can be observed that , PMSE power reaches a high value at time between 11:15 am to 11: 30 am with power almost 40dB. Below the heights 80Km , there is no such occurrence of echoes which is same for the heights between 100 km up to 110 km which is the height limit for my study. This shows that the prevalence of the PMSE exits in between 80-90 Km which is the mesopause height.

7.4 Doppler frequency

Higher variation of doppler frequency is mostly seen in the mesopause height. The figure 7.7 shows the variation from gate 1 to 53 each in total time. We can see the higher fluctuations of the doppler frequency at the some gates. Here each plots in array shows the variation in doppler frequency in each gate where x axis corresponds to time and y axis corresponds to the value of doppler frequency with last element containing no PMSE signal. To say it more clearly, the first element represents the variation of doppler frequency in 1st gate and so on.

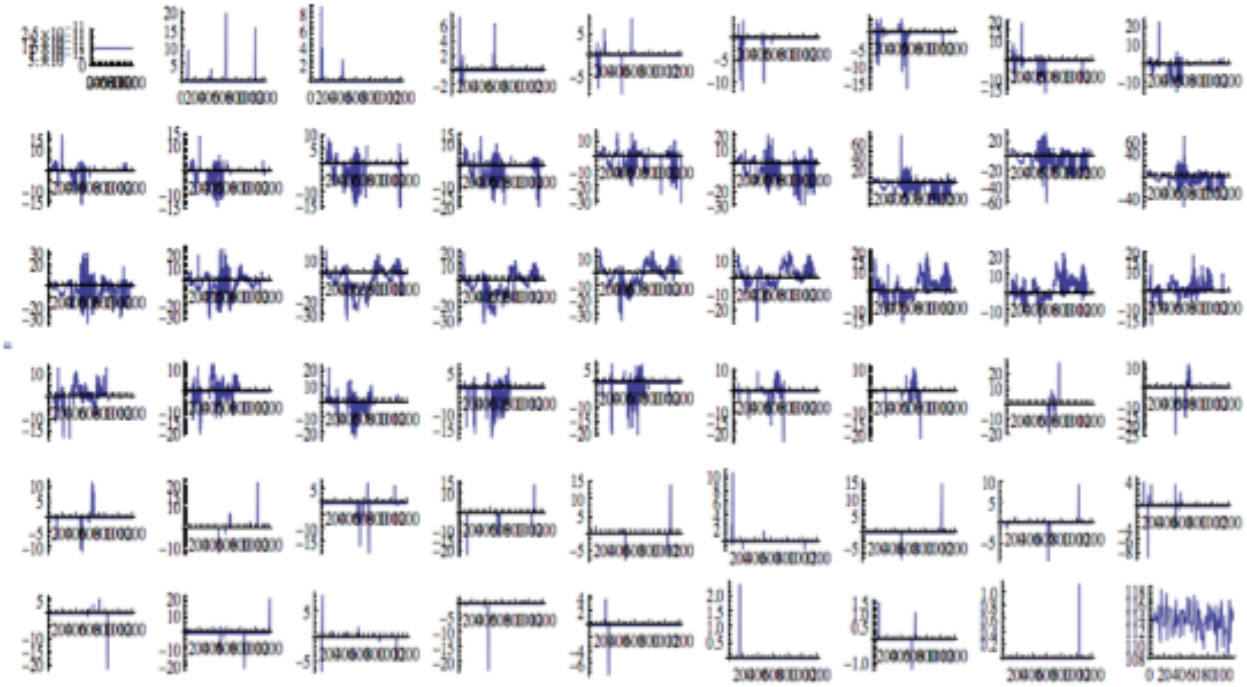

Figure 7.7: Doppler shift variations in hertz in all times shown in different gates.

Changing the doppler frequency to doppler velocity, I found out the plot of doppler velocity as a function of total time and height which is shown as below here.

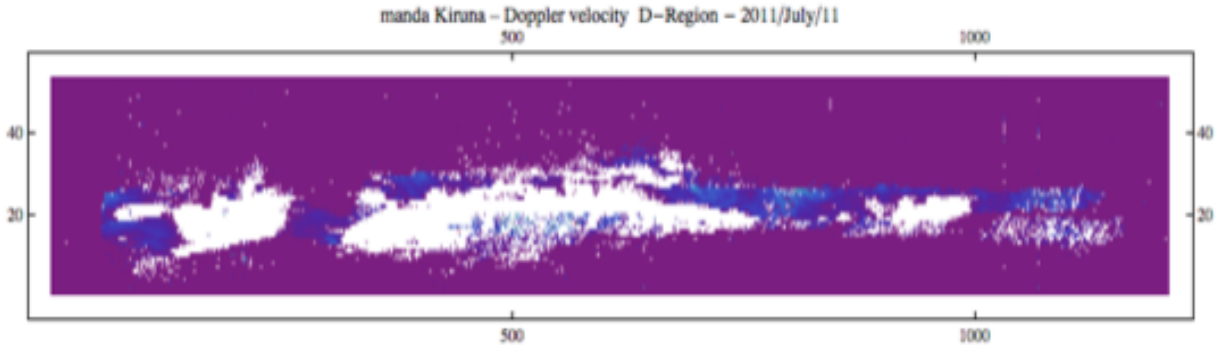

Figure 7.8: Variations in doppler velocity as a function of height and time.

7.5 Spectral Width

Similarly I found out the spectral width. In gates between 12 to 30, high dispersion of velocity of the echo is depicted. This suggests that the turbulence in this region of mesosphere is high resulting in such high dispersion which means that the spectral width of the spectrum that we have is of larger width in these heights. Here also, the 1st element of the plot shows the variation of spectral width in the first gate and so on, where the last plot in the last row is without PMSE signal. The X axis represents the time and Y axis shows the values of spectral widhts.

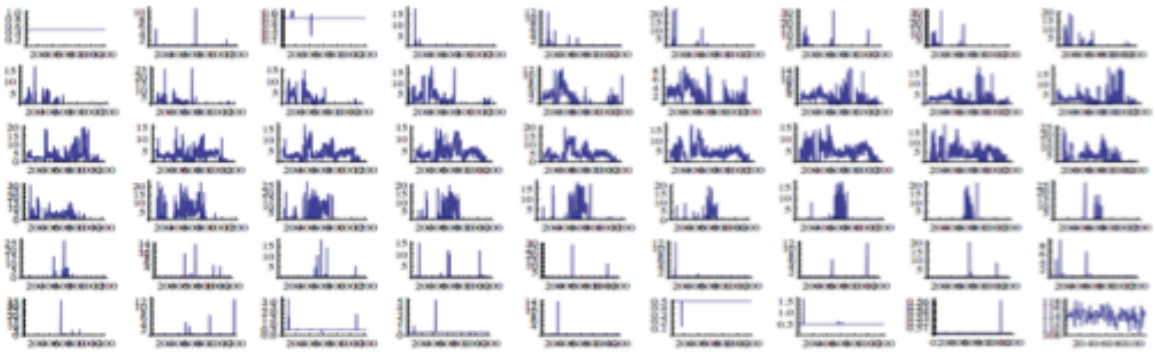

Figure 7.9: Variations of width in Hz in all times in different gates.

Figure 7.10 shows the spectral width(in Hz) varying along total time and height from which we can see the variation goes up to 20Hz.

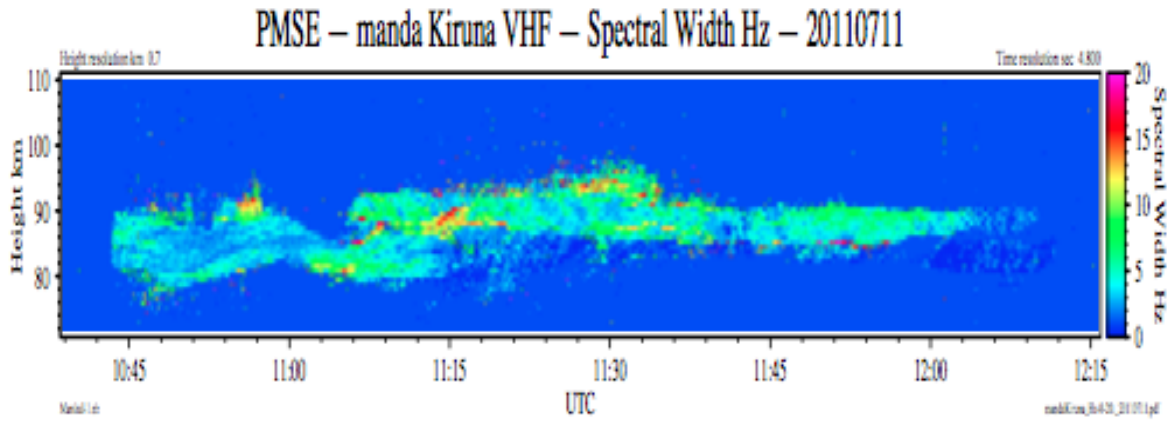

Figure 7.10: Variations in width in Hz as a function of height and time.

The figure 7.11 shows the variation of spectral width in m/s.

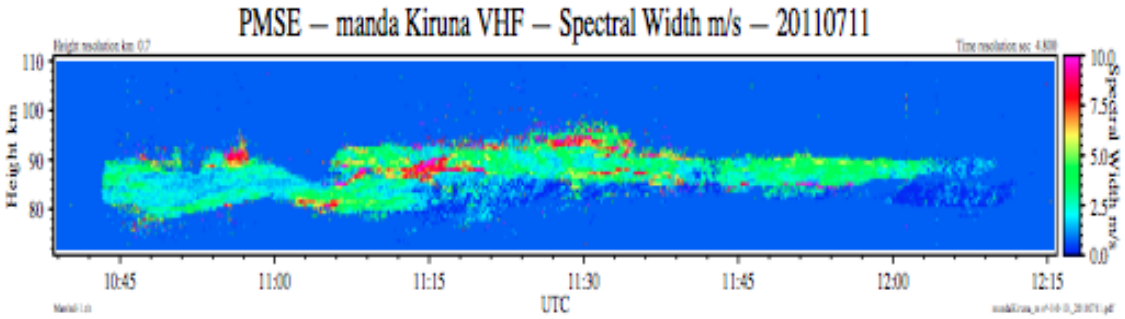

Figure 7.11: Variations in width in m/s as a function of height and time.

7.6 Dissipation rate

Dissipation varies as a function of width. So, with wider width, we obtain higher dissipation rate and vice-versa. The results obtained from dissipation here shows that the value can go up to 200mW/kg.

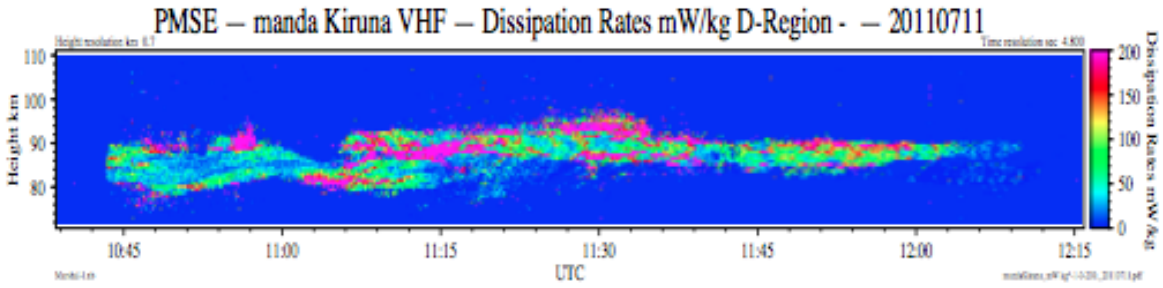

Figure 7.12: Dissipation of PMSE taken in all time at different gates.

The explanation given for existence of PMSE by the reduced diffusivity of electrons might work here because we saw the existence of PMSE even at smaller scales of dissipation evergy rate, ϵ.

Chapter 8

Conclusions and future recommendations

8.1 Conclusions

In my thesis I made a study on coherent scattered echoes ranging from heights around 70 Km up to 110 Km in the time interval between 10: 38 to 12:15 from the year 2011 july 11th during day time to study the turbulence in PMSE echoes.

I made an overview on the theory involved in creation of such enhanced PMSE echoes in VHF and UHF Bragg wavelength.Data analysis of such echoes obtained from EISCAT 3D demonstrator antenna array in Kiruna which receives from TrosmøVHF was analysed. With the main objective to see the turbulence footprints in PMSE, the dissipation rate was calculated. On the basis of dissipation rates, the nature of turbulence prevalent in such echoes in mesopause(between 80-90km) heights causing higher electron density fluctuations were discovered compared to other heights under observations.

From the plots made with different parameters like amplitude, width and doppler, it is clearly seen that the high variations in these quantities occur only in few gates. The radar coherent echoes that were received back have a high power reaching almost up to 40dB.

The irregularities retain the density fluctuations even when the dissipation energy rate reaches up to smaller scales i.e, 200mW/kg as shown in results which might be the due to to the presence of charged aerosols which decreases the electron diffusivity explained by the enhancement of Schmidt number. It is interesting to note that the values of dissipation predicts higher turbulence in PMSE layers.

8.2 Future recommendations

The main ground based techniques are EISCAT radars that are involved in investigating PMSE. Future investigations regarding PMSE can be focussed on improving its efficiency such as getting better data set for statistical analysis to get a more clear picture of these echoes.

Improving the radar efficiency to measure PMSE from all directions. This could give even more understanding on the nature of PMSE. In addition to that , the estimation of ice density could be made possible by improving the radar measurements.

So, with a strong and logical understanding of PMSE, observations of these layers can be an effective tool to understand the dynamics of the high atmosphere.

Bibliography

[1] R.R. Garcia and S. Solomon. The effect of breaking gravity waves on the dynamics and chemical composition of the mesosphere and lower thermosphere. *Journal of Geophysical Research*, 90(D2):3850–3868, 1985.

[2] S. Manabe and R.T. Wetherald. The effects of doubling the co2 concentration on the climate of a general circulation modell. *The Warming Papers*, page 138, 2011.

[3] F.J. Lübken, K.H. Fricke, and M. Langer. Noctilucent clouds and the thermal structure near the arctic mesopause in summer. *Journal of geophysical research*, 101(D5):9489–9508, 1996.

[4] V. Nussbaumer, KH Fricke, M. Langer, W. Singer, and U. Von Zahn. First simultaneous and common volume observations of noctilucent clouds and polar mesosphere summer echoes by lidar and radar. *Journal of geophysical research*, 101(D14):19161–19, 1996.

[5] U. von Zahn. Are noctilucent clouds a miner's canary for global change? *Eos, Transactions American Geophysical Union*, 84(28):261, 2003.

[6] H. Chandra and G. Dutta. Gravity waves in mesosphere. *Indian Journal of Radio and Space Physics*, 8:173–176, 1979.

[7] R.R. Garcia and S. Solomon. The effect of breaking gravity waves on the dynamics and chemical composition of the mesosphere and lower thermosphere. *Journal of Geophysical Research*, 90(D2):3850–3868, 1985.

[8] J.Y.N. Cho, C.M. Alcala, M.C. Kelley, and W.E. Swartz. Further effects of charged aerosols on summer mesospheric radar scatter. *Journal of Atmospheric and Terrestrial Physics*, 58(6):661–672, 1996.

[9] M. Rapp, F.J. Lübken, and TA Blix. The role of charged ice particles for the creation of pmse: a review of recent developments. *Advances in Space Research*, 31(9):2033–2043, 2003.

[10] M. Rapp, F.J. Lübken, P. Hoffmann, R. Latteck, G. Baumgarten, and T.A. Blix. Pmse dependence on aerosol charge number density and aerosol size. *Journal of Geophysical Research*, 108(D8):8441, 2003.

[11] J. Röttger, C. La Hoz, M.C. Kelley, U.P. Hoppe, and C. Hall. The structure and dynamics of polar mesosphere summer echoes observed with the eiscat 224 mhz radar. *Geophysical research letters*, 15(12):1353–1356, 1988.

[12] M.C. Kelley. Polar mesosphere summer radar echoes: Observations and current theories. *Reviews of Geophysics*, 31:243–265, 1993.

[13] V. Barabash. *Investigation of polar mesosphere summer echoes in northern Scandinavia*. PhD thesis, Umeå University, 2003.

[14] J. Bremer, P. Hoffmann, R. Latteck, and W. Singer. Seasonal and long-term variations of pmse from vhf radar observations at andenes, norway. *J. Geophys. Res*, 108(8):8438, 2003.

[15] F.J. Lfibken and J. Giebeler. Pmse layer. *Geophysical research letters*, 21(15):1651–1654, 1994.

[16] M. Rapp, I. Strelnikova, R. Latteck, P. Hoffmann, U.P. Hoppe, I. Häggström, and M.T. Rietveld. Polar mesosphere summer echoes (pmse) studied at bragg wavelengths of 2.8 m, 67cm, and 16cm. *Journal of Atmospheric and Solar-Terrestrial Physics*, 70(7):947–961, 2008.

[17] M. Rapp, J. Gumbel, FJ Lübken, and R. Latteck. D region electron number density limits for the existence of polar mesosphere summer echoes. *J. Geophys. Res*, 107(10.1029), 2002.

[18] M. Rapp, F.J. Lübken, et al. Polar mesosphere summer echoes (pmse): Review of observations and current understanding. *Atmospheric Chemistry and Physics Discussions*, 4(4):4777–4876, 2004.

[19] J.Y.N. Cho. An updated review of polar mesosphere summer echoes' observation, theory, and their relationship to. *Journal of geophysical research*, 102(D2):2001–2020, 1997.

[20] C. La Hoz, O. Havnes, LI Næsheim, and DL Hysell. Observations and theories of polar mesospheric summer echoes at a bragg wavelength of 16 cm. *Journal of geophysical research*, 111(D4):D04203, 2006.

[21] M. Rapp, I. Strelnikova, R. Latteck, P. Hoffmann, U.P. Hoppe, I. Häggström, and M.T. Rietveld. Polar mesosphere summer echoes (pmse) studied at bragg wavelengths of 2.8 m, 67cm, and 16cm. *Journal of Atmospheric and Solar-Terrestrial Physics*, 70(7):947–961, 2008.


UNIVERSITY
OF TROMSØ